

# Manufacturing Technologies and Applications

## MATECA



### Investigation of Joinability Of 25% Recycled Al6016 Sheets by Friction Stir Butt Welding at Different Tool Rotation Speed

Halil Kırdemir<sup>1,2\*</sup>, Cihan Yakupoğlu<sup>1,2</sup>, Faruk Varol<sup>2</sup>, Serkan Apay<sup>3</sup>

<sup>1</sup>Akpres Metal Yedek Parça Mak. San. Ve Tic. A.Ş., Ar-Ge, Sakarya, Türkiye

<sup>2</sup>Sakarya University of Applied Sciences, Graduate Education Institute Sakarya, Türkiye

<sup>3</sup>Düzce Üniversitesi, Mühendislik Fakültesi, Düzce, Türkiye

#### ABSTRACT

In this study, 2 mm thick Al6016 aluminum sheets containing 25% recycled material, commonly used in automotive body and chassis components, were joined using the friction stir welding (FSW) method in a butt joint configuration. Welding was performed on a mold milling machine using a conical tool made of 2379 grade steel, hardened to 62–64 HRC. Constant process parameters included a welding speed of 400 mm/min, tool plunge depth of 1.8 mm, shoulder diameter of 15 mm, and tool tilt angle of 90°. Tool rotation speeds were varied as 600, 1200, 1800, 2400, 3000, and 3600 rpm. Heat input was calculated for each condition. Mechanical performance of the joints was evaluated through tensile, bending, and hardness tests. Macro and microstructural examinations were also conducted, including fracture surface analysis. The highest tensile strength (214 MPa) was obtained at 1800 rpm, while the lowest (83 MPa) occurred at 600 rpm. In bending tests, no fractures were observed at 2400 and 3000 rpm, indicating good ductility and joint integrity. The highest hardness in the weld zone was 97.4 Hv, measured at 600 rpm. Macrostructural observations showed full penetration at all rotation speeds. Microstructural analysis revealed progressive grain refinement from the base metal toward the stir zone, confirming effective plastic deformation and recrystallization. The results demonstrate that tool rotation speed significantly affects joint quality. Optimal mechanical properties were achieved at intermediate speeds, particularly 1800 rpm, highlighting its potential for automotive applications involving recycled Al6016 sheets.

**Keywords:** Friction stir welding, Recycled Al6016, C2379

### %25 Geri Dönüştürülmüş Al6016 Sacların Sürtünme Karıştırma Alın Kaynağı İle Farklı Takım Devir Hızlarında Birleştirilebilirliğinin İncelenmesi

#### ÖZET

Bu çalışmada, otomotiv gövde ve şasi parçalarında yaygın olarak kullanılan, %25 geri dönüştürülmüş malzeme içeren 2 mm kalınlığındaki Al6016 alüminyum levhalar, alın birleştirme konfigürasyonunda sürtünme karıştırma kaynağı (FSW) yöntemiyle birleştirilmiştir. Kaynak işlemi, yüzey sertliği 62–64 HRC'ye kadar artırılmış konik geometri 2379 kalite çelikten üretilmiş bir takım ile kalıp freze tezgahında gerçekleştirilmiştir. Süreç parametrelerinden kaynak ilerleme hızı (400 mm/dak), takım daldırma derinliği (1.8 mm), omuz çapı (15 mm) ve takım eğim açısı (90°) sabit tutulmuştur. Takımın dönme hızı ise 600, 1200, 1800, 2400, 3000 ve 3600 dev/dak olacak şekilde değiştirilmiştir. Her hız için ısı girdisi hesaplanmıştır. Birleştirme kalitesi, çekme, eğme ve sertlik testleriyle değerlendirilmiştir. Ayrıca makro ve mikro yapısal incelemeler ile kırılma yüzey analizleri gerçekleştirilmiştir. En yüksek çekme dayanımı (214 MPa) 1800 dev/dak'ta elde edilirken, en düşük değer (83 MPa) 600 dev/dak'ta gözlemlenmiştir. Eğme testlerinde 2400 ve 3000 dev/dak'ta kırılma oluşmamış, bu da iyi süneklik ve kaynak bütünlüğü göstermiştir. Kaynak bölgesinde en yüksek sertlik 97.4 Hv ile 600 dev/dak'ta ölçülmüştür. Makroyapısal gözlemler, tüm dönme hızlarında tam nüfuziyet olduğunu göstermiştir. Mikroyapı incelemeleri, temel metalden kaynak bölgesine doğru ilerledikçe tane boyutunun incelendiğini ve etkin plastik deformasyon ile dinamik yeniden kristalleşmenin gerçekleştiğini ortaya koymuştur. Sonuçlar, takım dönme hızının birleştirme kalitesi üzerinde önemli etkileri olduğunu göstermektedir. Özellikle 1800 dev/dak'ta elde edilen mekanik performans, geri dönüştürülmüş Al6016 levhaların otomotiv uygulamalarında kullanım potansiyelini desteklemektedir.

**Anahtar Kelimeler:** Sürtünme karıştırma kaynağı, Geri dönüştürülmüş Al6016, C2379

#### 1. INTRODUCTION

The aluminum sheet used in automotive sector production is widely used in the industry due to its strength and lightness. The European Green Agreement aims to switch to a clean, circular economy and to

\*Corresponding author, e-mail: halil.kirdemir@akpres.com.tr

Received 19.08.2024; Revised 01.12.2024; Accepted 01.12.2024

<https://doi.org/10.52795/mateca.1553191>

To cite this article: H. Kırdemir, C. Yakupoğlu, F. Varol, S. Apay, Investigation of Joinability Of 25% Recycled Al6016 Sheets by Friction Stir Butt Welding at Different Tool Rotation Speed, Manufacturing Technologies and Applications, 6(1), (2025), 1-12.

increase the efficient use of resources by reducing climate change, biodiversity loss, recycling and pollution. Waste aluminum is chopped into small particles and then these pieces are melted in large furnaces. Thus, recycled aluminum, called aluminum, is obtained for reducing carbon emissions [1]. Sectors where friction stir welding is used include automotive, space, aviation, railway transportation, tool tips and ship industries. It is used in welding axles, shafts, pipes and transmission parts in automotive. This method is also one of the methods used in welding parts such as flanges, fittings, pipes and shafts in the machine manufacturing industry [2, 3].

In 1991, the British TWI (The Welding Friction stir welding, which was discovered by the Institute, is a new solid phase welding method that is still being researched a lot. This method was first used to join aluminum materials [4]. Friction stir welding is known as a solid state welding method. Unlike other welding methods, the parts to be joined are joined with the help of heat energy generated by mechanical rotation and applied pressure. In the method in question, the material is welded without melting, by undergoing plastic deformation with friction heat. Since no molten state is formed, no change occurs in the structure of the material. In this way, the mechanical properties of the material will not change after the welding process [4].

The use of the FSW method in industry seems to be increasing rapidly. When compared to gas metal arc welding methods, the absence of consumable elements such as protective gas, electrode or powder makes the method cheaper. The heat input generated in the joining of aluminum alloys with the fusion welding method can cause pore and crack formation in the weld seam as a result of the wide solidification temperature ranges of these alloys and their high thermal expansion. This situation causes the dissolution of hardening precipitates in the heat welding region in age-hardened aluminum alloys, which reduces the strength and hardness in the region under the effect of heat. In addition, welding causes mechanical incompatibility and changes the structural integrity. Today, many metal alloys such as aluminum, unalloyed steels, copper, stainless steels, magnesium and titanium can be joined successfully. The application of the FSW welding method is carried out using a special tip on conventional vertical milling machines [5].

It has been found that FSSW process improves the mechanical properties of the material for hardness, strength, fracture toughness, ductility, fatigue life, and corrosion resistance criteria [6]. The effects of tool-related friction stir welding parameters on different materials have been investigated. The parameters are: rotation speed, dwell time, vertical pressure, inclination angle, and tool geometry [7-11].

Barlas, Z. [12], The effect of tool inclination angle on tensile-shear failure load and weld zone characteristics for 1050 aluminum sheets welded by friction stir overlap welding was investigated. For this purpose, the tool inclination angle was varied from 0° to 5° under fixed other parameters such as tool geometry, tool rotation speed of 1200 rpm and tool movement speed of 30 mm/min. According to the general results, the tool inclination angle has a reasonable effect on the joint strength and weld defect formation. If the tool axis was perpendicular to the plate surface or a larger tool inclination angle was used, such configurations had a detrimental effect on the weld zone.

Barlas, Z. et al. [13], friction stir welding (FSW) parameters of tool rotation speed, tool inclination angle and tool rotation direction were used to join AlMg3 aluminum alloy (Al 5754) sheets with butt joints. When the tool was rotated counterclockwise, a solid and flawless weld was obtained with a tool rotation speed of 1100 rpm and a tool inclination angle of 2 degrees. The maximum tensile strength in the joint made with FSW parameters was 217 MPa, which was 14% lower than that of Al 5754 base metal. In this weld, a value closer to a symmetrical microhardness distribution was measured and the hardness values of the weld nugget region increased slightly, reaching approximately 82 HV.

De Caro, D. et al. [14], analyzed the sheet-aluminum 6181 alloy produced with different scrap content and compared it with a 6181 alloy from primary production. They showed that the alloys from secondary production contained higher amounts of manganese, iron and copper. They observed that the tensile properties did not change significantly, but a small increase in strength, probably related to the increased Cu and Mg content. However, they found the presence of defects in the form of inclusions at the fracture initiations, although the ductility did not change significantly.

D.N. Wang'ombe et al. [15], investigated the effects of feed and rotation speed on the tensile properties, microstructure and microhardness (HV) of extruded recycled Al 6061 alloy by friction stir welding. The studies on friction stir welding of recycled product mainly focused on the alloy content of primary Al 6061, which is different from that of Al 6061. The microstructure of the alloy consists of four zones, namely heat affected zone, thermo-mechanically affected zone, base metal and stirred zone. The average grain size of the gap was 93 µm. For the joints at 530 rpm and 100 mm/min, the average grain sizes were 7 µm in the stirred zone, 183 µm in the heat affected zone and 93 µm in the base metal. It was found that the tensile damage occurred in the heat affected zone exposed to high temperature. It was observed that the hardness decreased to a minimum in the heat affected zone, then there was a short increase in the thermo-mechanically affected

zone and reached another maximum in the stirred zone. The hardness developed in the machined zone was found to be inversely proportional to the tool rotation speed. It was found that the increase in speed increased the increasing heat which deteriorated the properties.

This study was carried out to investigate the mechanical and chemical structure properties of 6016 series sheets by using variable parameters in friction stir welding method for butt welding of 2 mm thick aluminum sheets with 25% recycled content. Test samples were prepared in accordance with TS EN ISO 25239 standards in the joints. For macro and micro imaging, the samples were sanded, polished and etched using Keller reagent (190 ml Pure Water + 3 ml HCl + 2 ml HF + 5 ml HNO<sub>3</sub>) reagents for 30 seconds. A 500x capacity optical microscope was used for imaging. Tensile strength, hardness measurements and bending tests of the trial joints were also performed.

## 2. MATERIAL AND METHOD

### 2.1. Materials Used in Experiments

25% recycled AL6016 alloy series 2 mm thick sheets and 2379 steel material are given in Table 1, and the chemical composition properties are given in Table 2.

Table 1. Mechanical properties of test specimens and agitator tool tip.

| Description | ( $\sigma_{Ak}$ ) | ( $\sigma_{max}$ ) | Elongation (%) | Hardness (HRC) |
|-------------|-------------------|--------------------|----------------|----------------|
| AL6016      | 103 MPa           | 182 MPa            | 24             | -              |
| 2379        | 1200 MPa          | 1590 MPa           | -              | 54-60          |

Table 2. Chemical composition (%) of test sample and stirrer tool tip.

| Description | Fe   | C        | Si        | Mn        | Cr          | Al   |
|-------------|------|----------|-----------|-----------|-------------|------|
| AL6016      | 0.24 | 0.001    | 0.57      | 0.14      | 0.03        | 98.3 |
| 2379        | 85   | 1.45-1.6 | 0.10-0.60 | 0.20-0.60 | 11.00-13.00 | -    |

Figure 1. a In accordance with the dimensions given, 2379 quality steel was processed in a lathe and heat treated to 60-64 HRC hardness. 2379 quality tool steel with 60-64 HRC was used in the experiments. The pin to be connected to the milling cutter has a diameter of 20 mm, a shoulder of 15 mm and a length of 90 mm. The mixing tip was manufactured from 2379 tool steel, whose melting point is approximately two and a half times higher than the melting point of the aluminum material. The pin sinking tip of 2379 tool steel was given a conical shape and the tip was machined at an angle of 10°.

In friction stir welding, a conical angle structure was created between the shoulder and the part of the mixer tip that will be connected to the vertical milling machine in order to reduce the heat generated by the mixer tip. The reason for this is to increase the contact area of the mixer tip with the air during welding and to discharge the heat generated by friction. The shoulder is the surface that sits on both plates during the friction stir welding stage. Since the shoulder part rubs against the contact surface of the two plates to be joined in friction stir welding, it provides the critical friction heat in friction stir welding. By covering the friction stir welding seam from the top, it minimizes the movement of the material moving upwards caused by the rotation of the tip during welding in Figure 1. b; in this direction, the material is pushed downwards by the shoulder. In Figure 1. c, the welding shoulder is ensured to sink approximately 1.8 mm into the surface of the material to be welded during the mixer tip welding process [16].

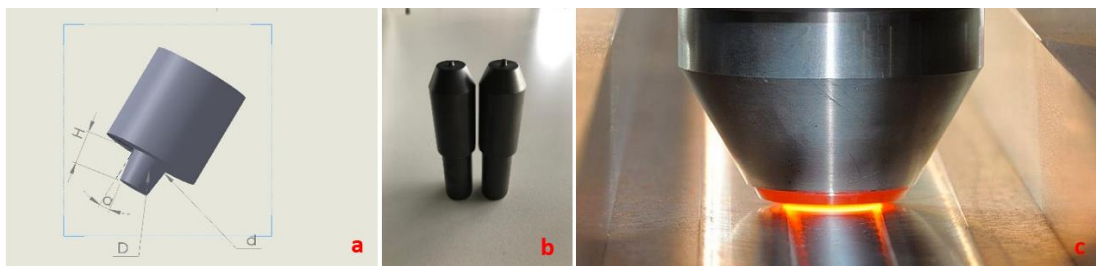


Figure 1. Tool pin desing (a), Tool pin (b), FSW butt weld (c).

## 2.2. Preparation of Test Samples

During friction stir welding, the aluminum alloy material was not subjected to any oxide removal before welding. The test samples were prepared from Al6016 sheets with dimensions of 2x1200x2400 mm by laser cutting. In friction stir welding, the sheets subject to the process were fixed and connected to the vertical milling machine table by means of connection shoes in a way that they would contact the edges to be welded. 2379 quality tool steel was specially turned and subjected to grinding process. The 25 mm body diameter mixer tip was connected to the vertical milling machine's vertical shaft and friction stir welding was applied to aluminum test sheets using the joining parameters shown in Table 3.

## 2.3. Applied Method

The joints were made by using the friction stir method in the butt-to-butt position on 25% recycled 2 mm 6016 Al series sheets with the condition of connecting to the milling machine by selecting the 2379 steel tool tip. 3 samples were prepared for each experiment for tensile and bending tests. Test samples were cut and prepared as 200x100 mm. Automatic operating mode was used in the milling machine system for applications. As seen in Figure 2, a special apparatus was manufactured to provide the butt-to-butt joining position and was positioned on the milling machine. Test samples of Al-Al plates joined at different rotation speeds (600 rpm, 1200 rpm, 1800 rpm, 2400 rpm, 3000 rpm, 3600 rpm) were prepared using laser cutting. Tensile test on ZwickRoell Z100 machine ISO 6892-1:2001 Bending tests were carried out according to the TSE EN ISO 5173:2010/A1 standard with a capacity of 50 kN Zwick 3-axis bending method was performed with Roell Z50 device. Hardness values of the samples were taken using Vickers method according to EN ISO 6507 standard with 100 gr load and pyramid indenter.



Figure 2. Milling machine (a), FSW application (b).

For micro and macro imaging, the samples were sanded, polished and etched using Keller reagent (190ml Pure Water + 3ml HCl + 2ml HF + 5ml HNO<sub>3</sub>) reagents for 30 seconds. A 500x capacity optical microscope was used for imaging. The applied source parameters are shown in Table 3.

## 2.4. Hardness Measurements

The hardness points of the joints are shown in Figure 3. Sample samples taken in all joining methods (Instron Wolpert) Hardness scanning was obtained at 1 mm intervals on the Vicker hardness tester. 100 gr. test load was applied in the hardness scannings (HV). While measuring the hardness; the base metal, joint area, thermomechanically affected area and weld metal values were scanned at equal intervals on both sides based on the center line of the weld.

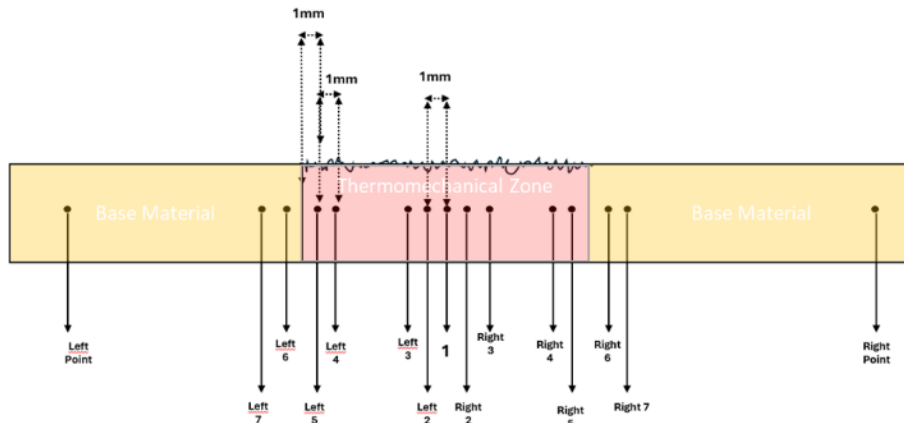


Figure 3. Hardness measurements.

Table 3. Friction stir welding joining parameters.

| Base Material | Thickness (mm) | Tool Speed (mm/dak) | Revolutions Per (Rpm) | Tool Material | Tool Geometry | Tool Pin Diameter (d: mm) | Tool Height (h: mm) | Shoulder Diameter (D: mm) | D/d | Tool Angle (o) | Joining Position |
|---------------|----------------|---------------------|-----------------------|---------------|---------------|---------------------------|---------------------|---------------------------|-----|----------------|------------------|
| AL 6016       | 2              | 400                 | 600                   | 2379          | Conical       | 3                         | 1.8                 | 15                        | 5   | 90             | Butt Joint       |
| AL 6016       | 2              | 400                 | 1200                  | 2379          | Conical       | 3                         | 1.8                 | 15                        | 5   | 90             | Butt Joint       |
| AL 6016       | 2              | 400                 | 1800                  | 2379          | Conical       | 3                         | 1.8                 | 15                        | 5   | 90             | Butt Joint       |
| AL 6016       | 2              | 400                 | 2400                  | 2379          | Conical       | 3                         | 1.8                 | 15                        | 5   | 90             | Butt Joint       |
| AL 6016       | 2              | 400                 | 3000                  | 2379          | Conical       | 3                         | 1.8                 | 15                        | 5   | 90             | Butt Joint       |
| AL 6016       | 2              | 400                 | 3600                  | 2379          | Conical       | 3                         | 1.8                 | 15                        | 5   | 90             | Butt Joint       |

### 2.5. Tensile Test Specimens

Tensile tests were carried out on the main material according to TS 138 (EN 10002-1) standard, and on the joined parts.-For the samples, 3 samples for each test were prepared in accordance with TS 287 (EN 895) standard. The technical drawing of the prepared sample and the tensile device test are shown in Figure 4. While the upper and lower clamps perform the tensile process by holding the two ends of the sample, the extensometer shows the changes in the length of a sample, also known as strain measurement.

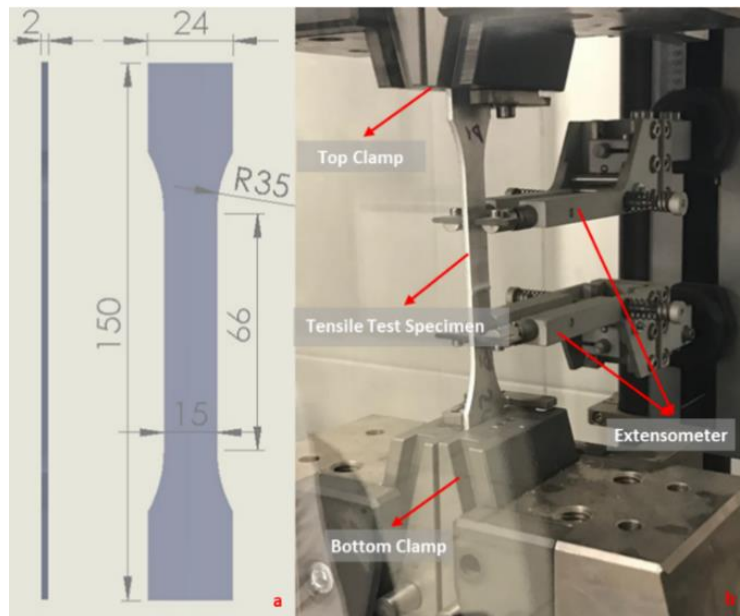


Figure 4. Sample technical drawing (a), Tensile test sample application (b).

## 2.6. Bending Test

Bending test aims to observe the cracks/breakages etc., that may occur in the weld area of the joined samples in the cold state. The bending test, which is applied according to the ISO 7438 standard, is performed by folding the plates with a thickness specified in Figure 5.a between two rounded supports with a pressure force by means of a bending mandrel of a certain diameter ( $d=2a$ ). The data obtained in the bending tests were carried out by preparing 3 samples from the base metal and for each parameter of the friction stir welding for a one-time comparison. The schematic and application representation of this machine is given in Figure 5.

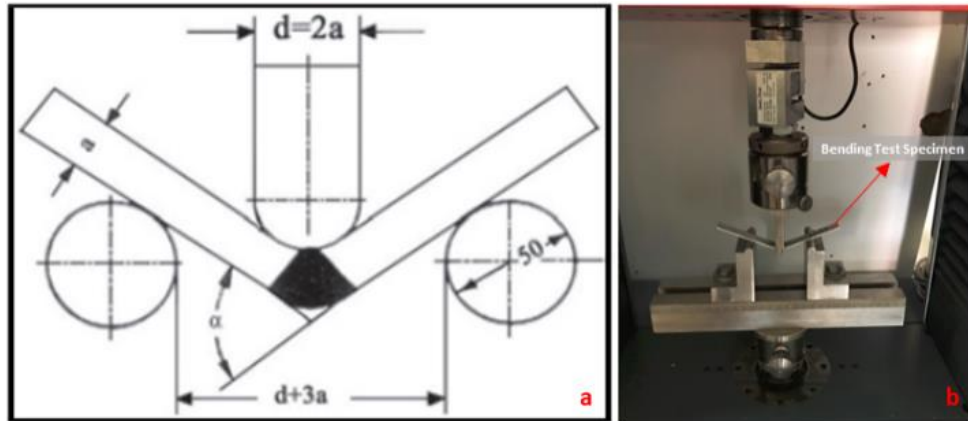


Figure 5. Schematic representation of bending test (a), Bending test specimen examples (b).

While the material is being folded during the bending process, after the first crack is seen, the load is removed and the bending angle of the piece is measured, or the cracks formed on the surface of the material folded 180° with a bending mandrel of a certain diameter and the appearance of its surface are examined.

## 3. RESULTS AND DISCUSSION

### 3.1. Heat Inputs and Tensile Test

The tensile test results of the joints made according to 6 different speeds, shown in Figure 6, were compared and it was seen that the highest strength was 214 MPa at 1800 rpm, the lowest strength was 83 MPa at 600 rpm. When compared with the base metal tensile strength, it was observed that the values were higher than the base metal at 1800, 2400 and 3000 rpm, but lower in other joints. Figure 6.a shows the images after the tensile test, and Figure 6.b shows the tensile strength ( $R_m$  (MPa)) values.

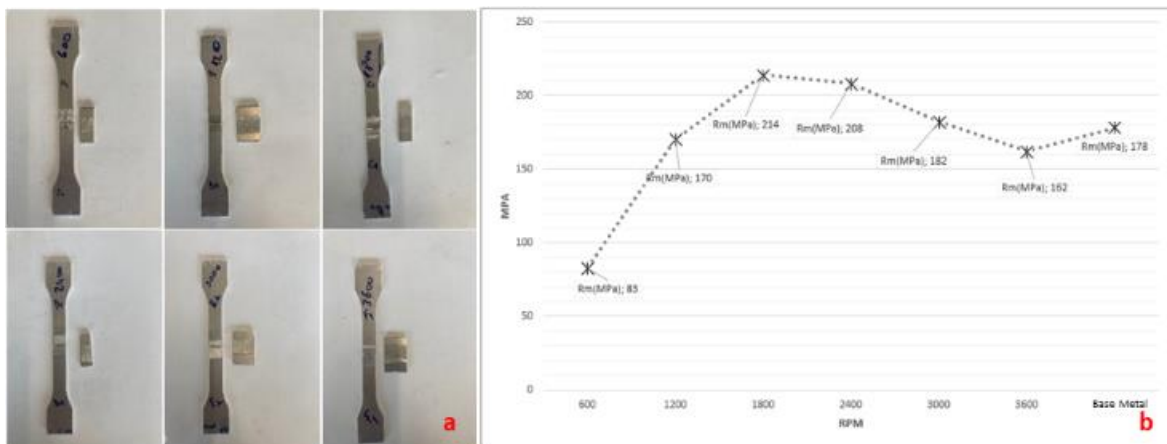


Figure 6. Tensile specimens and rupture zones (a), Rupture strength values graph (b).

Figure 7.a shows the heat input data for the joint at 6 different speeds. The heat inputs are calculated according to formula (1). In the FSW process, the weld heat input is affected by the tool rotation speed rather than the welding speed.

$T_m$  : melting point of the base metal,  
 $\omega$  : rotation speed,  
 $v$  welding speed  
 $\alpha$  : (0.04~0.06) and  $K$  (0.65~0.75) are constant

$$T = K \left( \frac{w^2}{v \times 10^4} \right)^{\alpha} T_m \tag{1}$$

As the speed of rotation increases on the fixed friction surface, the heat is observed to increase, the highest heat input is measured at 3600 rpm and 460 °C. Figure 7.b shows the instantaneous heat generation of the joints. The initial state is at room temperature, and the highest temperature values (375-460 °C) are observed between the 5th and 10th seconds. After the joint, a cooling curve is formed, reaching room temperature again at the 20th second. The highest temperature value is observed at 3600 rpm, while the lowest temperature value is observed at 600 rpm.

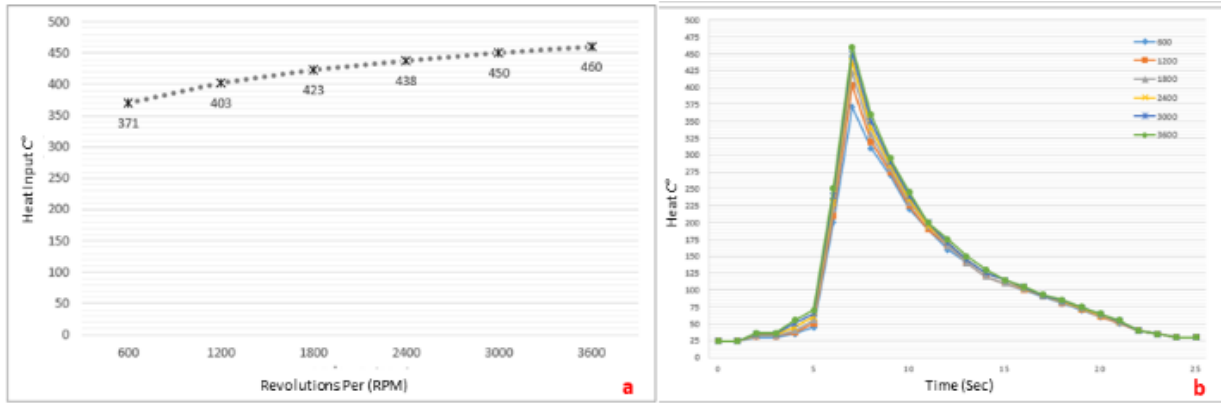


Figure 7. Heat input graph (a), Instantaneous heat generation (b).

The bending test results of the joints are shown in Table 4. The highest bending force was 3000 rpm and no fracture was observed in the weld area. Fractures were observed in the weld areas at 600, 1200, 1800 and 3600 rpm and it was determined that it was unsuccessful.

Table 4. Load and bending force of joints.

| Sample | Type | $E_f$<br>GPa | $\sigma_{fC}$<br>MPa | $\sigma_{fM}$<br>MPa | $\epsilon_M$<br>mm | L<br>mm | h<br>mm | b<br>mm |
|--------|------|--------------|----------------------|----------------------|--------------------|---------|---------|---------|
| 1      | 3600 | 34.5         | 7.43                 | 184                  | 2.0                | 60      | 2       | 15.2    |
| 2      | 3000 | 33.2         | 254                  | 310                  | 12                 | 60      | 2       | 15.2    |
| 3      | 2400 | 35.2         | 227                  | 296                  | 15                 | 60      | 2       | 15.2    |
| 4      | 1800 | 40.9         | 228                  | 269                  | 7.7                | 60      | 2       | 15.2    |
| 5      | 1200 | 32.4         | 231                  | 296                  | 14                 | 60      | 2       | 15.2    |
| 6      | 600  | -1.3         | 6.99                 | 65.3                 | 0.32               | 60      | 2       | 15.2    |

Although the same bending force (296 MPa) was reached at 1200 and 2400 rpm, fractures occurred in the 1200 rpm weld zone, and fractures also occurred at 600, 1800 and 3600 rpm, but it was observed that there was no fracture in the 2400 and 3000 rpm weld zone and the result was successful. It was observed that the mixing and heat input changed in direct proportion to the tool rotation speed, and the fractures that occurred in joints other than 2400 and 3000 rpm were; jointing could not be achieved at 600 rpm, and partial joint areas were formed in joints at 1200 and 1800 rpm. It was observed that the heat input was maximum at 3600 rpm and it was determined that deteriorations (dimensional variation) occurred in the main material during cooling with heat input. It was determined that the fracture zones that progressed from the crack zone formed in the joint zone for all joints were brittle fractures. It was observed that the hardness values in all joint areas were close to each other. The bending forces of the joints are shown in Figure 8. a. The bending application is shown in Figure 8 (b).

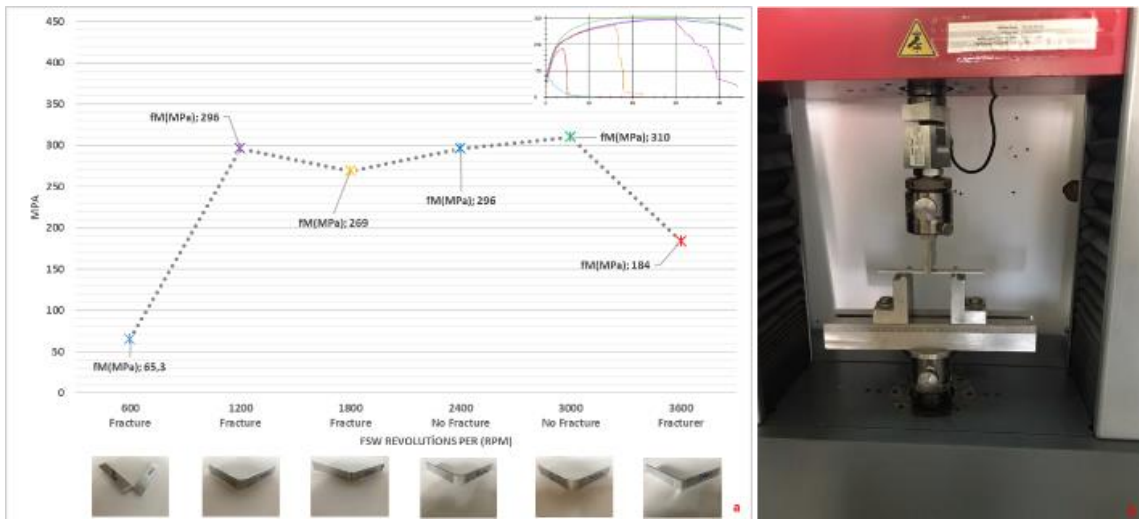


Figure 8. Bending force graph (a), Bending test application example (b).

### 3.2. Heat Inputs and Tensile Test

The current state of the base material to be joined affects the hardness behavior after FSW. In this study, the hardness line was determined along the cross-section of the weld zone and was monitored sequentially. Al6016 base metals have an average hardness value of  $107 \pm 2$  HV for 2 mm sheet thickness. Figure 9 shows that the hardness of the weld zone of FSW joints decreases significantly at all applied rotation speeds due to the frictional heat generated during FSW processes causing annealing of the Al6016 base metal. For each butt welded joint between the weld zone, minimum hardness values were observed in the thermomechanical zone due to the grain structure and excessive aging effects. In contrast, Ahmed et al. reported that the presence of high hardness areas in the thermomechanical zone is mainly due to the dynamic recrystallized fine grain structure and the redeposition process that may occur during the cooling cycle [17]. It can be attributed to the high heat intensity generated as a result of plastic deformation during the FSW process. In addition, the variations in tensile shear are probably due to the increased thermal softening (changing hardness values) in the thermomechanical area due to the increased heat input and the decrease in the thickness of the layers under the shoulder with pressure. The hardness values after the joints were taken as rank hardness (HV) values from the main material, the joint area and the thermomechanically affected areas and are given in Table 5. The hardness data of all these joints were seen as the highest value of 105 HV in the main material. The hardness values decrease towards the joint area. The lowest value of the joint area was determined as 97.4 HV. The rank hardness values of 6 different joints are shown in Figure 9.

Table 5. Hardness (HV) values at reference points.

| Rpm  | Left Point | Left2 | Left3 | Left 4 | Left 5 | Left 6 | Left 7 | 1    | Right 2 | Right 3 | Right 4 | Right 5 | Right 6 | Right 7 | Right Point |
|------|------------|-------|-------|--------|--------|--------|--------|------|---------|---------|---------|---------|---------|---------|-------------|
| 600  | 105        | 86.4  | 91.5  | 90.2   | 86.2   | 97.4   | 96.8   | 92.1 | 83.7    | 96.3    | 85.9    | 91.8    | 102     | 106     | 103         |
| 1200 | 68.4       | 80.8  | 84.9  | 83.4   | 81.9   | 72.1   | 74     | 77.9 | 79.1    | 85      | 75.1    | 71      | 73.9    | 77.3    | 86.7        |
| 1800 | 90         | 75.6  | 77    | 71.6   | 71.5   | 71.3   | 74.8   | 74.4 | 77.2    | 79.4    | 71.9    | 73.8    | 81.9    | 83.9    | 86.4        |
| 2400 | 93.8       | 84    | 91.5  | 84.7   | 81.1   | 83.9   | 92.9   | 91.3 | 82.4    | 81.5    | 74.2    | 76      | 87.4    | 89.2    | 104         |
| 3000 | 85.4       | 78.7  | 86.6  | 76.7   | 73.6   | 76.5   | 82.5   | 77.8 | 86.9    | 82.5    | 86.2    | 85.8    | 74.7    | 78.2    | 94.4        |
| 3600 | 87.1       | 84.5  | 85.5  | 83.4   | 84.6   | 85     | 81.5   | 74.5 | 88.2    | 73      | 76.4    | 74      | 65.6    | 66.8    | 78.9        |

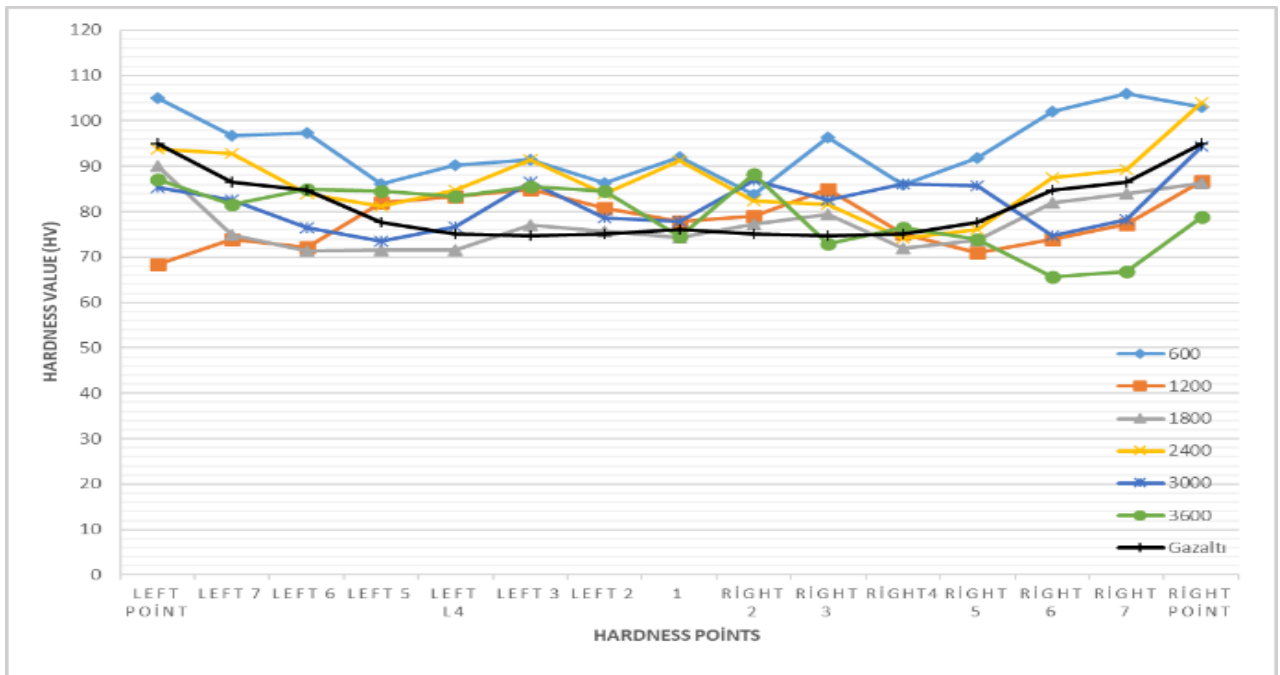


Figure 9. Hardness values.

### 3.3. Examination of Macro Structures

During friction stir welding of aluminum, the immersed stir tip in the welding region releases the mixing energy in the fusion region and ensures that two different aluminums are mixed together. Figure 10 shows macro images of 6 different joints. Material accumulation (mm), joint adequacy (mm), measurement variation ( $^{\circ}$ ), crack formation (mm) and penetration (mm) values are shown in the joint regions. Material accumulation and joint insufficiency were observed at 600 rpm. The joint with the highest measurement variation was 1800 rpm. Crack formation was observed in every joint and was observed most at 2400 rpm. It was observed that sufficient penetration levels occurred at all rpm speeds. While it was observed that the highest tensile strength value was at 1800 and 2400 rpm speeds, it was observed that the tensile strength decreased at other parameter values.

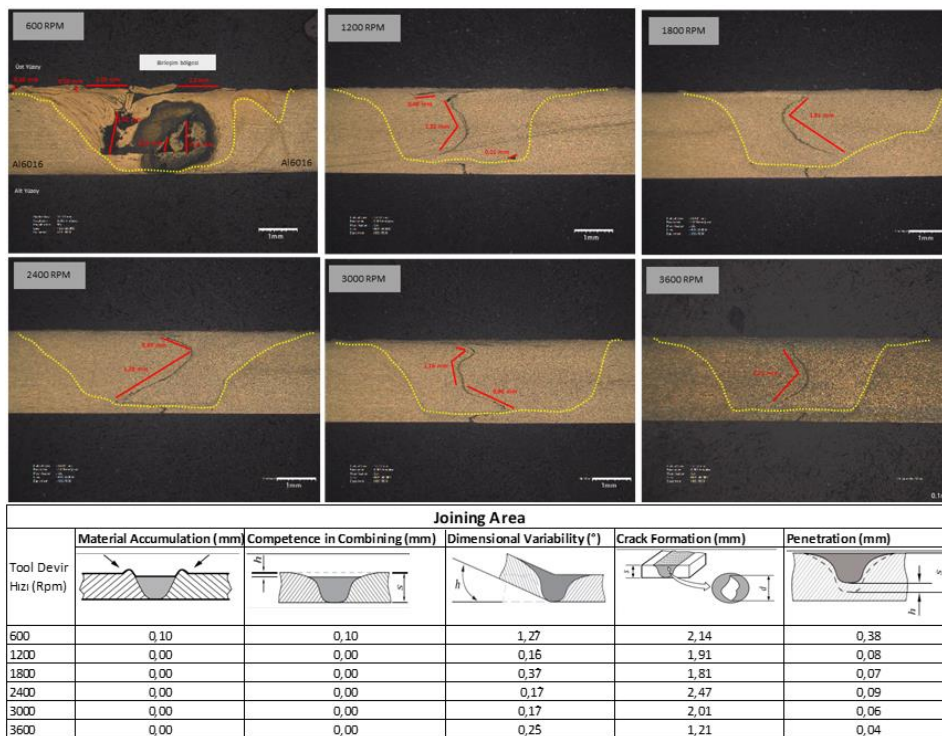


Figure 10. Macro images and joint region defects.

When the fracture surfaces are examined in Figure 11, it was determined that the mixer tip could not provide sufficient mixing during the joint and created thin film-shaped capillary cracks in the inner region of the joint. In addition, since the 600 rpm joint conditions could not be provided in the joints at 6 different speeds, it was not determined that the fracture was in an irregular line. For the joints at other speeds, the same geometry as the crack fault formed in the weld zone and the fracture progress were observed. It was determined that the fracture points occurred in the joint zone where there were micro cracks.

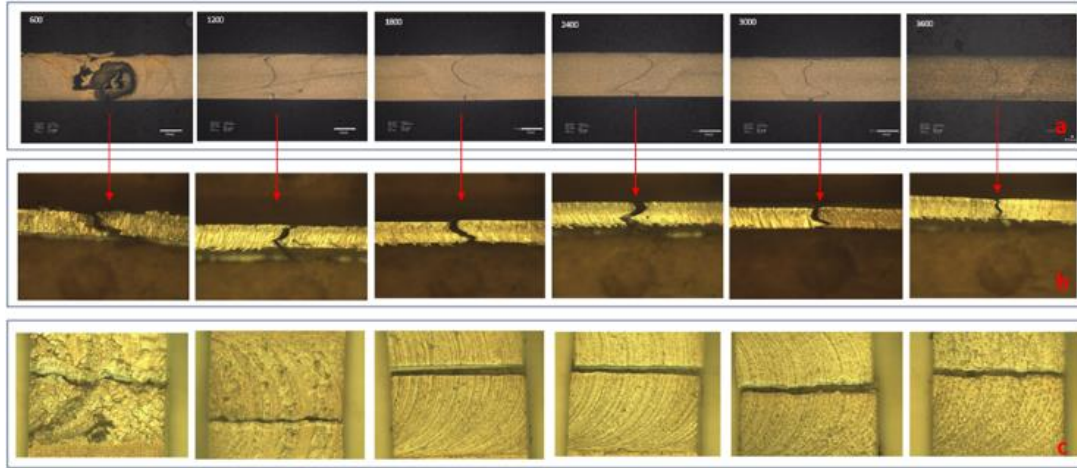


Figure 11. Joining zone microcrack (a), Joining zone front view after fracture (b), Joining zone top view after fracture (c).

### 3.4. Examination of Micro Structures

When the microstructures and grain sizes between the plates are examined, it shows the effect of heat input on the average thickness of the layer formed between the aluminum and the fusion zone during the friction stir welding process. The thickness of the layer has formed a coarse-grained layer at different speeds since the cooling rate of the FSW source changes in different regions with the change of the welding speed. Depending on the speed values of the mixer tip, the grain thickness is different, and the grain size changes not only with the mixer tip but also with the change of the speed. This affected the mechanical properties of the welded area between the samples after joining. The formation of high temperatures causes intense plastic deformation, which occurs in the material during joining. As a result, fine-structured recrystallized grains are formed. Thanks to the fine-grained microstructure formed, appropriate mechanical properties are obtained in the welding area [18].

Mixing tip, shoulder size and shape are important for mixing and heat input generation. The shoulder also provides compression of the material volume exposed to heat. Another function of the tool is to move the material by mixing it. Tool design and process loads affect the homogeneity of microstructure and properties. A concave shoulder and threaded cylindrical pins are often used. When the critical effect of tool geometry on metal flow is considered, the fundamental correlation between weld microstructure and material flow varies for each tool [19].

In Figure 12, micro images of the joints made at 2400 rpm were taken and it was determined that the grain structure became thinner from the base metal towards the joint area.

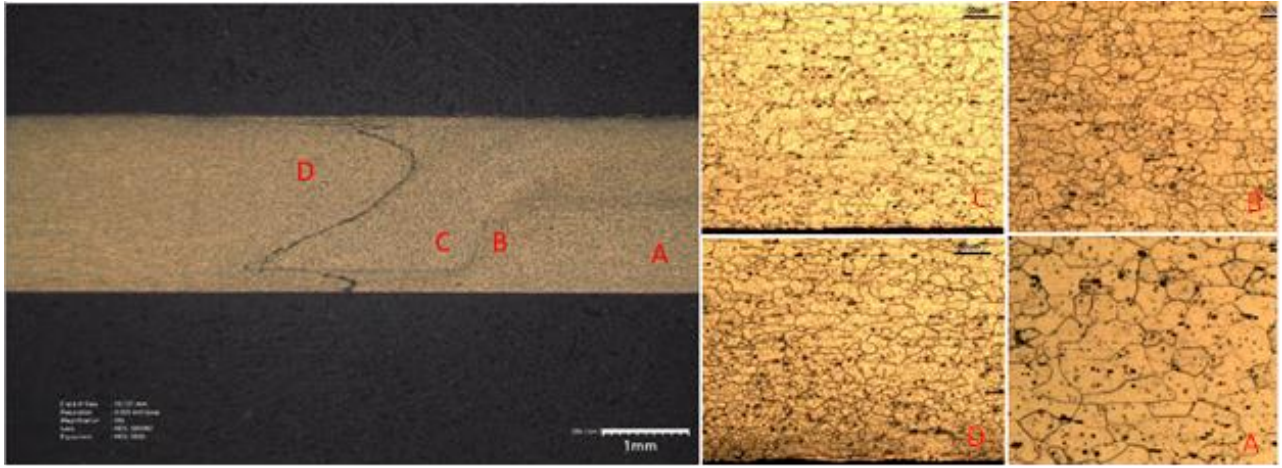


Figure 12. Comparison of micro images.

#### 4. CONCLUSIONS

The joinability of 25% recycled Al6016 sheets by friction stir butt welding was investigated at 6 different tool speeds from 600 to 3600 rpm.

The highest tensile strength value was found to be 214 MPa at 1800 rpm and the lowest value was 83 MPa at 600 rpm at a feed rate of 400 mm/min.

No fracture was observed after the bending test of the specimens joined at 2400 and 3000 rpm. In the bending tests applied to the specimens joined at other rotational speeds, the weld failed by breaking from the weld seam.

The highest results of the joint hardness values were measured as 97.4 HV at 600 rpm rotational speed.

When the macrostructures were analysed, the joint with the highest measured change was 1800 rpm. Crack formation was observed at all joints, with the highest occurrence at 2400 rpm. Adequate penetration levels were found to occur at all rpm speeds.

When the micro images of the joints made at 2400 rpm were analysed, it was observed that the grain structure became thinner from the base metal to the joint region.

#### ACKNOWLEDGMENT

This study was supported by Ak-Pres Otomotiv A.Ş.

#### REFERENCES

- [1] E. Özdemir, B. Ercan, Avrupa Yeşil mutabakatının enerji sektörüne ve otomotiv endüstrisine etkileri ve sonuçları, *EJOSAT*, 190-202 (2023), <https://doi: 10.31590/ejosat.1280352>.
- [2] A.W. El-Morsy, M. Ghanem, H. Bahaitham, Effect of friction stir welding parameters on the microstructure and mechanical properties of AA2024-T4 Aluminum Alloy, *Engineering, Technology & Applied Science Research*, 8 (2018) 2493-2498, <https://doi: 10.48084/etasr.1704>.
- [3] S.S. Yılmaz, B.S. Ünlü, M. Uzkut, D. Ertürk, Alüminyum alaşımlarında sürtünme karıştırma kaynağı ve uygulamaları, *Mühendis ve Makina*, 57 (2016) 676.
- [4] C. Meran, M. Colak, Tool holder design for friction stir welding, *Journal of the Faculty of Engineering and Architecture of Gazi University*, 23 (2008) 671-679.
- [5] B. Çevik, Y. Ozcatalbas, I. Uygur, 7075 Alüminyum alaşımının sürtünme karıştırma kaynağı ile birleştirilmesi, *International Conference on Welding Technologies and Exhibition*, May 2012, 396-376.
- [6] I. Charit R.S. Mishra, Low temperature superplasticity in a friction-stir-processed ultrafine grained Al-Zn-Mg-Sc alloy, *Acta Materialia*, 53(15) (2005) 4211-4223.
- [7] J. Gronostajski, H. Marciniak, A. Matuszak, New methods of aluminium and aluminium-alloy chips recycling, *Journal of Materials Processing Technology*, 106(1) (2000) 34-39.
- [8] Y. Li, L.E. Murr, J.C. McClure, Flow visualization and residual microstructures associated with the friction-stir welding of 2024 aluminum to 6061 aluminum, *Materials Science and Engineering: A*, 271 (1999) 213-223.
- [9] Ş. Mert, S. Mert, Sürtünme karıştırma nokta kaynak yönteminin incelenmesi”, *Düzce University Journal Of Science And Technology*, 2 (2013) 26-35.
- [10] M. Peel, A. Steuwer, M. Preuss, P.J. Withers, Microstructure, mechanical properties and residual stresses as a function of welding speed in aluminium AA5083 friction stir welds, *Acta Materialia*, 51(16) (2003) 4791-4801, [https://doi: 10.1016/S1359-6454\(03\)00319-7](https://doi: 10.1016/S1359-6454(03)00319-7).

- [11] S. Malopheyev, I. Vysotskiy, V. Kulitskiy, S. Mironov, R. Kaibyshev, Optimization of processing-microstructure-properties relationship in friction-stir welded 6061-T6 aluminum alloy, *Materials Science and Engineering: A*, 662 (2016) 136-143.
- [12] Z. Barlas, The influence of tool tilt angle on 1050 aluminum lap joint in friction stir welding process, *Acta Physica Polonica A*, 132(2017) 679-681.
- [13] Z. Barlas, U. Ozsarac, Effects of FSW parameters on joint properties of AlMg3 alloy, *Welding journal*, 91 (2012) 16-22.
- [14] D.De Caro et al., Effect of recycling on the mechanical properties of 6000 series aluminum-alloy sheet, *Materials*, 16 (2023) 6778, [https://doi: 10.3390/ma16206778](https://doi.org/10.3390/ma16206778).
- [15] H. Dawood et al., Effect of friction stir welding on microstructure and mechanical properties of the 6061 aluminium alloy/15vol % SiC p reinforcement, *IOP Conference Series: Materials Science and Engineering*, 870, (2020) 012162, [https://doi: 10.1088/1757-899X/870/1/012162](https://doi.org/10.1088/1757-899X/870/1/012162).
- [16] G. am, Friction stir welding: A novel welding technique developed for al-alloys, 46 (2005) 30-39.
- [17] M. Ahmed, B. Wynne, W. Rainforth, A. Addison, J. Martin, P. Threadgill, Effect of tool geometry and heat input on the hardness, grain structure, and crystallographic texture of thick-section friction stir-welded aluminium, *Metallurgical and Materials Transactions A*, 50 (2018) 271-284.
- [18] A. Őik, İ. Ertürk, M. Önder, A study into effects of different parameters on mechanical properties in friction stir welding of AA 2024 aluminium alloy, *Pamukkale University Journal of Engineering Sciences*, 16(2) (2010) 139-147.
- [19] . Batuk, H. Demirtaş, Sürtünme karışırma kaynađı ile birleřtirilmiř 6061 alüminyum alařımlı sacların mekanik özellikler yönünden incelenmesi, *Manufacturing Technologies and Applications*, 4(3) (2023) 167-178, [https://doi: 10.52795/mateca.1393930](https://doi.org/10.52795/mateca.1393930).